

Characterization of genetic lesions in rhabdomyosarcoma using a high-density single nucleotide polymorphism array

メタデータ	言語: English 出版者: 公開日: 2021-06-28 キーワード: 作成者: Nishimura, Riki, Takita, Junko, Sato-Otsubo, Aiko, Kato, Motohiro, Koh, Katsuyoshi, Hanada, Ryoji, Tanaka, Yukichi, Kato, Keisuke, Maeda, Daichi, Fukayama, Masashi, Sanada, Masashi, Hayashi, Yasuhide, Ogawa, Seishi, 前田, 大地 メールアドレス: 所属:
URL	https://doi.org/10.24517/00062685

This work is licensed under a Creative Commons Attribution-NonCommercial-ShareAlike 3.0 International License.



Characterization of genetic lesions in rhabdomyosarcoma using a high-density single nucleotide polymorphism array

Riki Nishimura,¹ Junko Takita,^{2,9} Aiko Sato-Otsubo,³ Motohiro Kato,⁴ Katsuyoshi Koh,⁴ Ryoji Hanada,⁴ Yukichi Tanaka,⁵ Keisuke Kato,⁶ Daichi Maeda,⁷ Masashi Fukayama,⁷ Masashi Sanada,³ Yasuhide Hayashi⁸ and Seishi Ogawa³

¹Department of Pediatrics; ²Cell Therapy and Transplantation Medicine; ³Cancer Genomics Project, Graduate School of Medicine, University of Tokyo, Tokyo; ⁴Saitama Children's Medical Center, Saitama; ⁵Kanagawa Children's Medical Center, Kanagawa; ⁶Ibaraki Children's Hospital, Ibaraki; ⁷Department of Pathology, Graduate School of Medicine, University of Tokyo, Tokyo; ⁸Gunma Children's Medical Center, Gunma, Japan

(Received February 21, 2013/Revised March 19, 2013/Accepted March 30, 2013/Accepted manuscript online April 11, 2013/Article first published online May 23, 2013)

Rhabdomyosarcoma (RMS) is a common solid tumor in childhood divided into two histological subtypes, embryonal (ERMS) and alveolar (ARMS). The ARMS subtype shows aggressive clinical behavior with poor prognosis, while the ERMS subtype has a more favorable outcome. Because of the rarity, diagnostic diversity and heterogeneity of this tumor, its etiology remains to be completely elucidated. Thus, to identify genetic alterations associated with RMS development, we performed single nucleotide polymorphism array analyses of 55 RMS samples including eight RMS-derived cell lines. The ERMS subtype was characterized by hyperploidy, significantly associated with gains of chromosomes 2, 8 and 12, whereas the majority of ARMS cases exhibited near-diploid copy number profiles. Loss of heterozygosity of 15q was detected in 45.5% of ARMS that had been unrecognized in RMS to date. Novel amplifications were also detected, including *IRS2* locus in two fusion-positive tumors, and *KRAS* or *NRAS* loci in three ERMS cases. Of note, gain of 13q was significantly associated with good patient outcome in ERMS. We also identified possible application of an ALK inhibitor to RMS, as *ALK* amplification and frequent expression of *ALK* were detected in our RMS cohort. These findings enhance our understanding of the genetic mechanisms underlying RMS pathogenesis and support further studies for therapeutic development of RMS. (*Cancer Sci* 2013; 104: 856–864)

Rhabdomyosarcoma (RMS) is the most common soft tissue sarcoma in children. Two major histological subtypes are recognized: alveolar (ARMS) and embryonal (ERMS). The ERMS subtype (approximately 60% of all RMS cases) is usually a localized disease with a favorable prognosis, typically occurring in younger children.⁽¹⁾ It presents mostly as a disease of the head, neck or genitourinary tract.⁽¹⁾ In contrast, the ARMS subtype, which accounts for approximately 20% of RMS, commonly involves the extremities in older children, exhibiting aggressive clinical behavior with frequent metastatic diseases.⁽¹⁾ Approximately 75% of ARMS exhibit characteristic chromosomal translocations, t(2;13)(q35;q14) and t(1;13)(p36;q14), which generate aberrant fusion transcription factors *PAX3-FOXO1* and *PAX7-FOXO1*, respectively.^(2,3) Loss of heterozygosity (LOH) at 11p15.5 is a common chromosomal aberration in ERMS as well as other pediatric tumors, for example, Wilms tumor and hepatoblastoma.⁽⁴⁾ According to previous reports using array-based comparative genomic hybridization, numerical changes primarily involving gains of chromosomes 2, 8 and 12 are generally associated with ERMS, and ARMS are typically characterized by genomic amplifications^(5–8) including co-amplifications of *PAX3/7* and *FOXO1*

loci in fusion-positive tumors.^(5,7–9) Although these genetic findings suggest that the two subtypes represent discrete clinicopathological entities, their molecular basis has not been completely elucidated.

In the present study, we performed high-density single nucleotide polymorphism (SNP) array analysis of 55 RMS specimens with the aim of identifying characteristic genomic profiles including allelic imbalances as well as novel candidate gene targets in RMS.

Materials and Methods

Patient samples and cell lines. A total of 55 RMS specimens including 47 fresh tumors (11 ARMS, 31 ERMS, one unclassified RMS and three unknown RMS) and eight cell lines (ERMS: RD, RMS, SCMC-RM2, SJRH1 and ICH-ERMS-1; ARMS: SJRH4, SJRH18 and SJRH30) were analyzed in the present study (Table 1). In one ERMS case, two different pieces of the same tumor block (E16-1, E16-2) were analyzed to investigate intratumor heterogeneity in RMS. The RMS cell lines were either established in our laboratory (SCMC-RM2) or kindly provided by Dr A.T. Look (SJRH series), Dr K. Yokomori (RMS), Dr A. Inoue (RD) and Dr K. Kato (ICH-ERMS-1). SCMC-RM2 was established from bone marrow tumor cells obtained during a relapse in case E23, and ICH-ERMS-1 was from the primary tumor of case E11. Tumor samples were obtained from multiple hospitals in Japan, including Saitama Children's Medical Center, Kanagawa Children's Medical Center and Ibaraki Children's Hospital. Diagnosis of RMS was established using light microscopy, immunohistochemistry and/or gene tests. The present study was approved by the Ethics Committee of University of Tokyo (approval number 1598) and informed consent was obtained from parents.

SNP array analysis. The DNA extracted from RMS samples was subjected to SNP array analysis using Affymetrix GeneChip 50K *Hind* or 250K *Nsp* (Affymetrix, Inc., Santa Clara, CA, USA) according to the manufacturer's protocol. Copy number analyzer for GeneChip/allele – specific copy number analysis using anonymous references (CNAG/AsCNAR) was used for subsequent informatics analysis for SNP array data, which enabled accurate detection of allelic status without paired normal DNA even in the presence of up to 70–80% normal cell contamination.^(10,11) Amplification was defined as

⁹To whom correspondence should be addressed.
E-mail: jtakita-ky@umin.ac.jp

Table 1. Clinical information on the rhabdomyosarcoma samples examined using a single nucleotide polymorphism array

Case ID/cell line	Sex	Histological subtype	Stage	Outcome	Fusion gene	50K/250K array
A1	M	ARMS	4	Alive	<i>PAX3/FOXO1</i>	250K
A2	F	ARMS	4	Dead	<i>PAX3/FOXO1</i>	250K
A3	F	ARMS	Unknown	Unknown	<i>PAX7/FOXO1</i>	250K
A4	F	ARMS	1	Alive	<i>PAX3/FOXO1</i>	250K
A5	M	ARMS	Unknown	Unknown	<i>PAX7/FOXO1</i>	250K
A6	M	ARMS	Unknown	Alive	<i>PAX7/FOXO1</i>	250K
A7	F	ARMS	4	Dead	<i>PAX7/FOXO1</i>	250K
A8	F	ARMS	1	Dead	<i>PAX3/FOXO1</i>	250K
A9	M	ARMS	3	Dead	Unknown	250K
A10	M	ARMS	4	Alive	<i>PAX3/FOXO1</i>	250K
A11	F	ARMS	3	Dead	Negative	250K
E + 1	F	ERMS	4	Alive	<i>PAX7/FOXO1</i>	250K
E + 2	F	ERMS	4	Dead	<i>PAX3/FOXO1</i>	250K
E + 3†	F	ERMS	Relapse, metastasis	Dead	<i>PAX7/FOXO1</i>	250K
E + 4	F	ERMS	3	Alive	<i>PAX3/FOXO1</i>	250K
E + 5	M	ERMS	1	Dead	<i>PAX3/FOXO1</i>	250K
E + 6	M	ERMS	3	Dead	<i>PAX7/FOXO1</i>	250K
E1	F	ERMS	1	Alive		250K
E2	M	ERMS	3	Dead		250K
E3	F	ERMS	Unknown	Dead		250K
E4	M	ERMS	3	Alive		250K
E5	M	ERMS	4	Alive		250K
E6	F	ERMS	Relapse	Alive		250K
E7	M	ERMS	Unknown	Alive		250K
E8	F	ERMS	3	Alive		250K
E9	M	ERMS	4th relapse	Alive		250K
E10	M	ERMS	4	Dead		250K
E11	M	ERMS	4	Dead		250K
E12	F	ERMS	1	Alive		250K
E13	F	ERMS	3	Dead		250K
E14	F	ERMS	3	Dead		250K
E15	F	ERMS	3	Alive		250K
E16	M	ERMS	3	Unknown		250K
E17	M	ERMS	3	Dead		250K
E18	F	ERMS	3	Alive		250K
E19	F	ERMS	3	Dead		250K
E20	F	ERMS	1	Alive		250K
E21	M	ERMS	3	Unknown		250K
E22	F	ERMS	Unknown	Dead		250K
E23	F	ERMS	4	Dead		250K
E24	M	ERMS	3	Unknown		250K
E25	F	ERMS	1	Dead		250K
UC1	M	Unclassified	4	Dead		250K
U1	M	Unknown	Unknown	Dead		250K
U2	F	Unknown	Unknown	Unknown		250K
U3	F	Unknown	Unknown	Unknown		250K
SJRH18		ARMS			<i>PAX3/FOXO1</i>	50K
SJRH30		ARMS			<i>PAX3/FOXO1</i>	50K
SJRH4		ARMS			<i>PAX3/FOXO1</i>	250K
SCMC-RM2		ERMS			<i>PAX3/FOXO1</i>	250K
RD		ERMS				50K
RMS		ERMS				50K
SJRH1		ERMS				50K
ICH-ERMS-1		ERMS				250K

†This case was diagnosed as ARMS after re-evaluation of the paraffin section. ARMS, rhabdomyosarcoma with alveolar subtype; ERMS, rhabdomyosarcoma with embryonal subtype; F, female; ID, identification; M, male.

an inferred copy number of ≥ 5 and gain was defined as that of 3–4. The array data have been deposited in the Gene Expression Omnibus at NCBI (GEO; www.ncbi.nlm.nih.gov/geo) with accession number GSE41263.

Analyses of gene mutations/expressions. Reverse transcription polymerase chain reaction (RT-PCR) was used for detecting

PAX3/PAX7-FOXO1 and *PAX3-NCOA1/NCOA2* fusion transcripts and expressions of *ALK*, *GPC5* and *IRS2*. All exons of *GPC5*, the pleckstrin homology and phosphotyrosine binding domains of *IRS2* and the juxtamembrane and kinase domains of *ALK* were examined for mutations using direct sequencing. The primers and PCR conditions are listed in Supporting Information

Table S1. Mutation analysis of *ALK* was performed as described previously.⁽¹²⁾

Fluorescence *in situ* hybridization (FISH). Two-color FISH was performed for confirmation of gene amplification of *SJRH18* at *PAX3* and *FOXO1* loci using SureFISH probe (Agilent Technologies, Cedar Creek, TX, USA) according to the manufacturer's instructions. Probe number: *PAX3* G100099G (green); and *FOXO1* G100128R (red).

Sensitivity to *ALK* inhibitors and cell viability assay. Sensitivity of RMS cell lines to *ALK* inhibition was tested using the *ALK* inhibitors TAE684, 2,4-PDD and crizotinib. *SJRH1*, *SJRH4*, *SJRH18*, *SJRH30*, *RD* and *RMS* were cultured in the medium containing serial dilutions of each *ALK* inhibitor or vehicle (DMSO) and cell viability was evaluated using CellTiter-Glo Luminescent Cell Viability Assay (Promega, Madison, WI, USA). The IC_{50} was calculated for each cell line using nonlinear regression (variable slope) with the top fixed at 100 and the bottom at 0, using *GRAPHPAD PRISM 5* software (GraphPad, La Jolla, CA, USA).⁽¹³⁾ Semi-quantitative RT-PCR was performed for analysis of *ALK* expression followed by comparison between the *ALK* expression level and IC_{50} of each *ALK* inhibitor in RMS cell lines. The *ALK* inhibitors were provided by Astellas Pharma Inc. (Tokyo, Japan).

Statistical analysis. Fisher's exact test was used to evaluate the differences in chromosomal copy number changes between

ARMS and ERMS or the correlation between copy number changes and prognosis in each subgroup.

Results

Subtype-specific copy number profiles in RMS. Of the 55 RMS samples, 43 tumor specimens and all eight cell lines had one or more copy number alterations and/or allelic imbalances (Fig. 1). All but one hyperploidy case were near-diploid in ARMS, whereas 68% of the ERMS cases exhibited hyperploidy profiles, significantly associated with gains of chromosomes 2, 8 and 12 (chromosome 2, $P = 0.0042$; chromosomes 8 and 12, $P = 0.00076$) (Figs 1 and S1), which is consistent with the published data.^(5,7-9) Most cases (16/19) with gains of chromosome 2, 8 or 12 showed a concurrent increased number of all three chromosomes and nine of 18 cases with a gain of chromosome 8 exhibited an increased number of both alleles. In ERMS, 66.7% of the survival cases represented a gain of chromosome 13q, which was detected in 9.1% cases with a poor prognosis (Fig. S2). The difference reached statistical significance ($P = 0.0094$).

Loss of heterozygosity with or without copy number losses. Loss of heterozygosity is a common finding in cancer genomes that can be comprehensively detected using a SNP array, even when not accompanied by copy number losses.⁽¹⁴⁾ In fact,

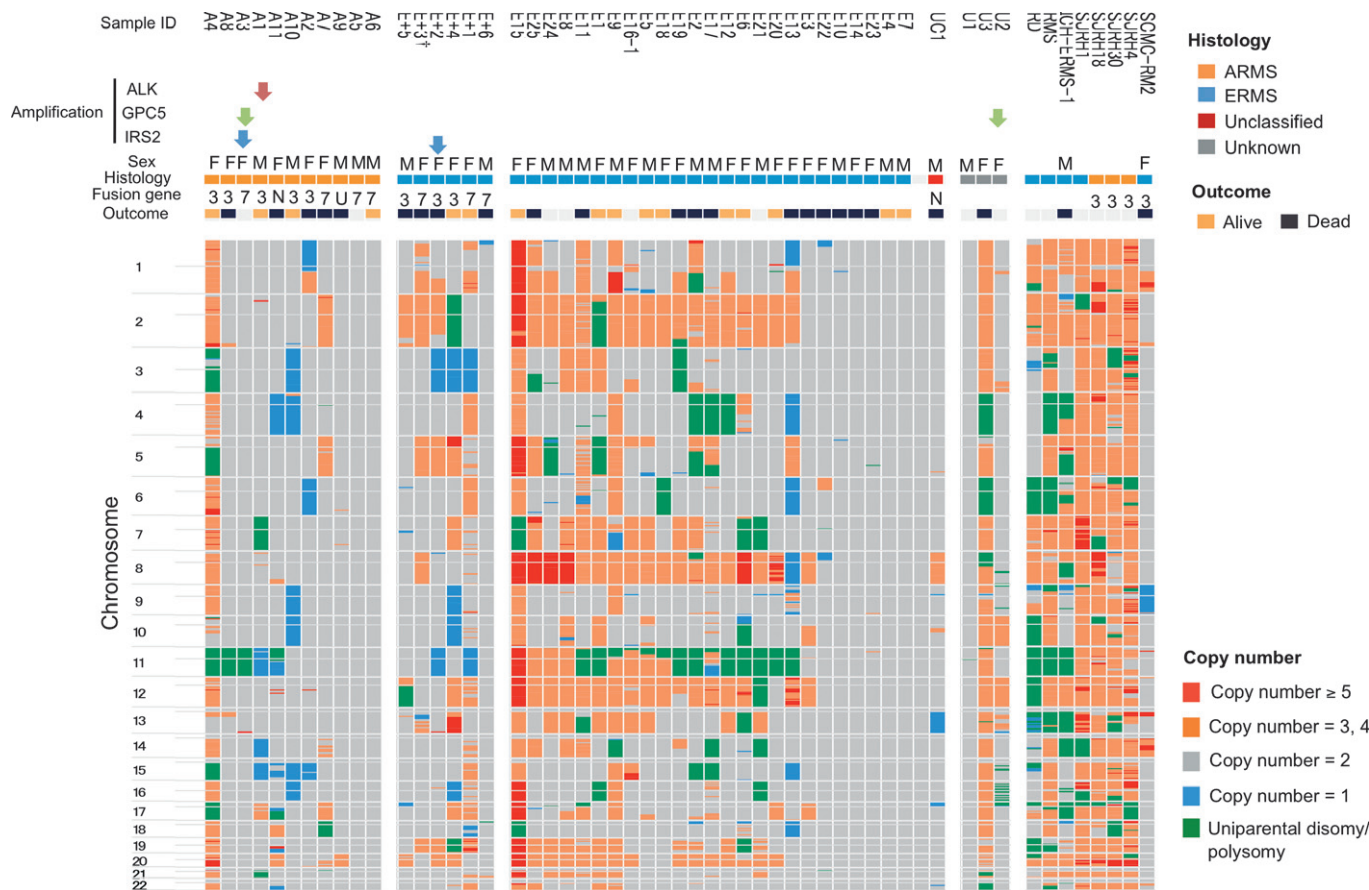


Fig. 1. Overview of copy number changes and allelic imbalances detected using a single nucleotide polymorphism (SNP) array in 46 RMS tumors and eight cell lines. Copy number data were separated based on fresh tumors of each subgroup and cell lines. Each row corresponds to chromosome 1–22 and each column indicates the affected region of the chromosomes in a single specimen. Genetic lesions, histological information and outcome are color coded according to the legend and clustering was performed using visual inspection. Sample name and clinical information are indicated at the top of the graph. Amplifications (*ALK*, *GPC5* and *IRS2*) are indicated by the red, green and blue arrows, respectively. This figure was drawn using CNAGgraph software. †This case was diagnosed as ARMS after re-evaluation of the paraffin section. 3, *PAX3-FOXO1*; 7, *PAX7-FOXO1*; ARMS, rhabdomyosarcoma with alveolar subtype; ERMS, rhabdomyosarcoma with embryonal subtype; F, female; M, male; N, fusion-negative; U, unknown fusion status.

65.7% of all LOH regions detected in the present RMS cohort were retained neutral or increased copy numbers (uniparental disomy/polysomy). As shown in Figure 2, LOH patterns were relatively comparable in both subgroups. The most frequent LOH was 11p not only in ERMS (56.0%) but also in ARMS (45.5%), and the second was 15q detected in 21.9% of all RMS, which was more common in ARMS (45.5%). 15q LOH has not been described previously in RMS, of which the minimal overlapping regions were 15q11.2–q13.3 and 15q21.3–q25.3, containing several candidate genes such as *TRPM1*, *SMAD3* and *PML*. However, we could not find any clinical impact of 15q LOH in ARMS in the present study. As previously reported,⁽¹⁵⁾ deletion of *CDKN2A/2B* was found in six cases (A10, E + 4, E + 5, E + 6, E13 and E23), deletions of *NF1* in three ERMS cases (E6, E15 and E25), which occurred concurrently with amplification of *MDM2*, and 17p LOH including *TP53* locus in four cases (A4, E + 5, E11 and U2) in our 46 RMS cases.

Gains/amplifications in RMS. The most frequently amplified regions in RMS were *PAX3/PAX7* and *FOXO1* loci constituting RMS-specific translocations (Fig. 3a), which were also found in samples with unknown fusion status. For the detection of *PAX3/PAX7-FOXO1* transcripts, RT-PCR was performed in samples for which cDNA were available, resulting in positive for the same fusion that was changed in the SNP array analysis. Genomic amplification of *PAX3-FOXO1* in SJRH18 was confirmed using FISH (Fig. 3b). As unbalanced translocations were also observed in *PAX3-FOXO1*-positive samples, such alterations at the fusion points were found in 17 of 19 fusion-positive RMS (Table S2). In the present RMS

cohort, seven ERMS samples represented amplifications or unbalanced translocations at *PAX3/7* and *FOXO1* loci, suggesting the presence of RMS-specific fusion genes. As the fusion transcripts are found exclusively in ARMS, these fusion-positive ERMS were separated from the ERMS group in the present study. Among the fusion-positive ERMS, histological re-evaluation could be done in only one case (case E + 3) and therefore this case was considered to be an alveolar subtype.

Other recurrent amplifications included the following: the *MYCN* locus at 2p24 found in five of 46 primary RMS cases (three ARMS and two ERMS); 7q21 contained *CDK6* in two cases (one ERMS and one unknown); 13q31 including *GPC5* and *miR-17-92* in two cases (one ARMS and one unknown); and 12q13–q21.2 in six cases (three ARMS and three ERMS), which constitutes various combinations of three separate amplicons including 12q13.2–q14.1, 12q15 and 12q15–q21.2, as has been described in past reports^(6,8) (Fig. 3c). Another amplification found in an ARMS case contained the *ALK* locus at 2p23 (Fig. 3d).

Although novel amplifications were found mostly in a single case (Table S3), two recurrent regions were detected in the present study: one located at 13q33–q34 including *IRS2* found in one ARMS and one fusion-positive ERMS (Fig. 4a), and the other at 1p13.2–q12 contained *NRAS* found in two ERMS (one case exhibited gain) (Fig. 4b). In addition, we identified one ERMS case with *KRAS* amplification, which has not been described previously in RMS (Fig. 4c). An amplification of 8q13 found in an unclassified RMS involved the *NCOA2* gene, which has been reported as a recurrent fusion partner of *PAX3*

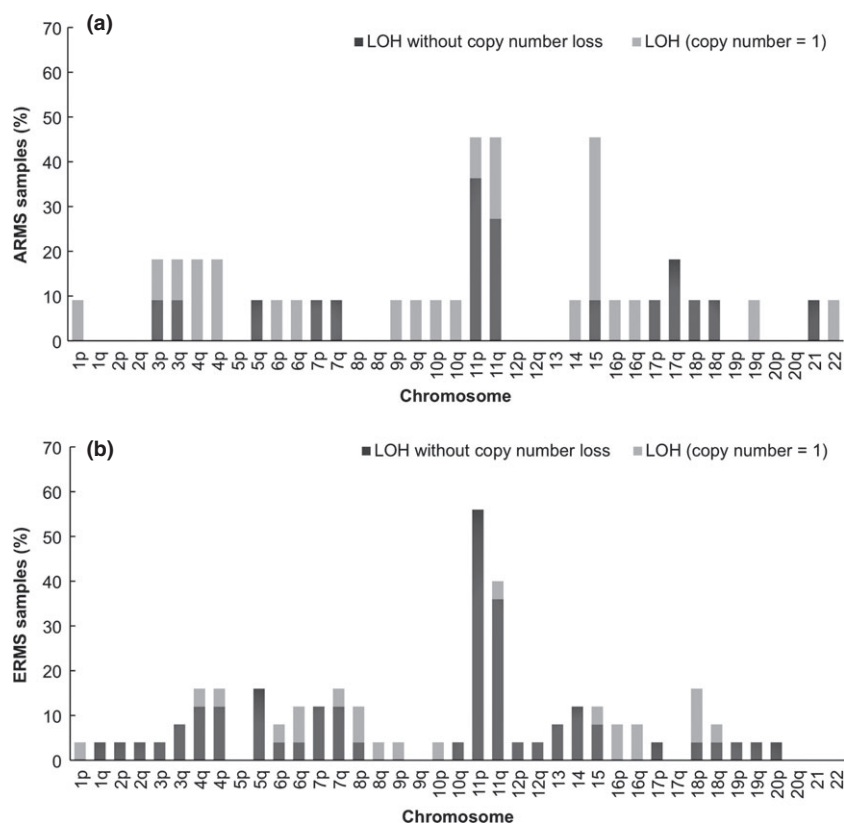


Fig. 2. Allelic imbalances detected in ARMS and ERMS. Distributions and frequencies of loss of heterozygosity (LOH) are demonstrated using bar graphs. Uniparental disomy/polysomy and LOH (copy number = 1) are indicated separately by different shades of gray. The data of fusion-positive ERMS and cell lines are not included in the graphs. (a) Summary of 11 ARMS tumors. (b) Summary of 21 ERMS tumors. ARMS, rhabdomyosarcoma with alveolar subtype; ERMS, rhabdomyosarcoma with embryonal subtype.

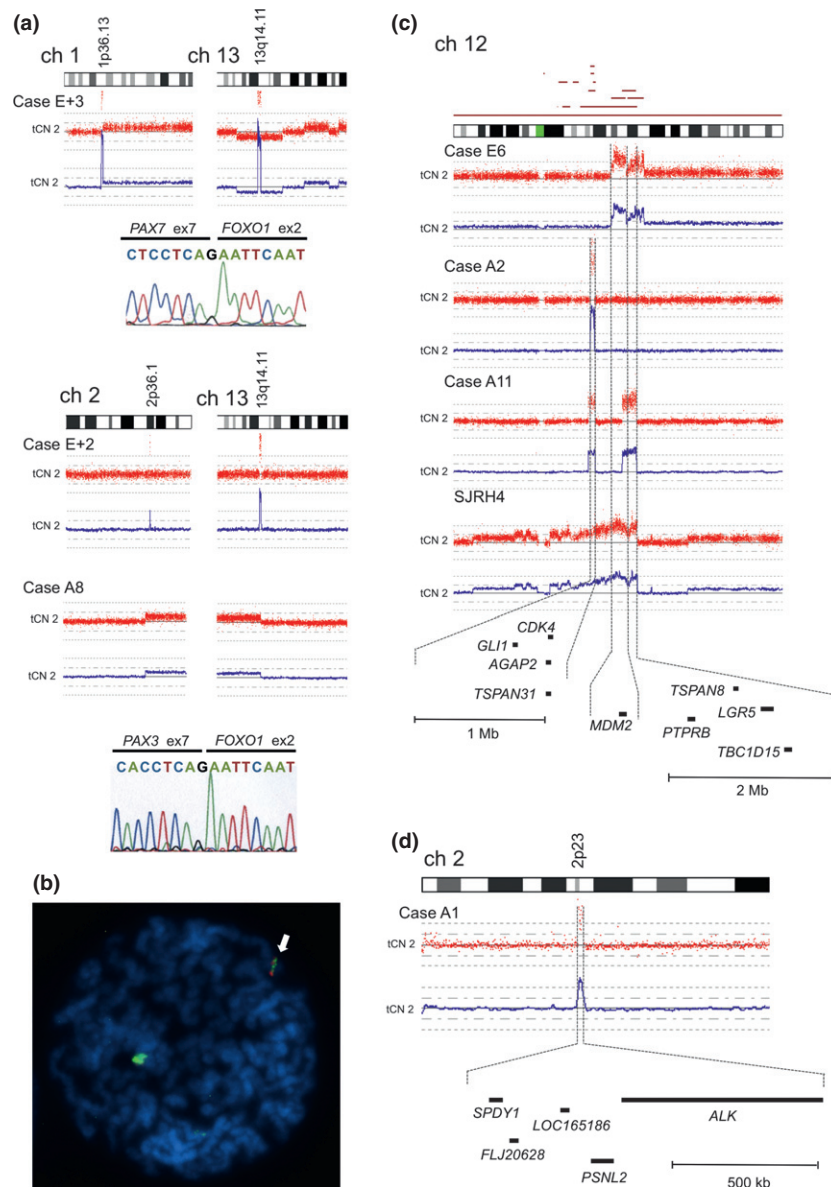


Fig. 3. Representative results of amplifications detected in rhabdomyosarcoma (RMS). In the images of single nucleotide polymorphism (SNP) array, the red dots demonstrate the raw copy number and the blue lines below the red dots indicate a moving average of 10 SNP. (a) Upper image represents amplifications of *PAX7* and *FOXO1* loci in a fusion-positive ERMS. This case was diagnosed ARMS after re-evaluation of the paraffin section. Lower images show the *PAX3* and *FOXO1* loci in two cases: case E + 2 with amplification and case A8 with unbalanced translocation. Breakpoint regions of each chimeric transcript were confirmed using direct sequencing. (b) FISH of *SJRH18*, a cell line with the *PAX3-FOXO1* fusion gene. The *PAX3* spanning probe set in red and the *FOXO1* spanning probe set in green reveals the presence of juxtaposed red and green signals with a homogeneous staining region pattern (arrow), consistent with the RT-PCR and SNP array data. (c) Amplified regions around 12q13–q21.1 are depicted in detail from high-resolution copy number analysis. In the upper panel, each horizontal red line above the chromosome ideogram illustrates the amplified regions (copy number ≥ 5) in a single tumor, revealing all amplified regions in the present cohort, and below this are the patterns and degree of amplification in four representative samples. At the bottom of the figure, representative genes contained in each common region are indicated by a black bar. (d) Amplification of *ALK* detected in an ARMS case. ARMS, rhabdomyosarcoma with alveolar subtype; ERMS, rhabdomyosarcoma with embryonal subtype; tCN, total copy number.

in a subset of ARMS,^(16,17) whereas no amplification at the *PAX3* locus and no *PAX3-NCOA2* fusion transcript were detected in this case.

Characteristic copy number profiles in RMS cell lines. In eight RMS-derived cell lines analyzed, all but one of them were grossly hyperploid and displayed more complex structural abnormalities than tumor samples (Fig. 1). In comparison between cell lines and the corresponding original tumors, that is, case E11 and ICH-ERMS-1, case E23 and SCMC-RM2 established from relapsed tumor cells, many differences were indeed found between them, which contained not only additional

but also disappeared changes, e.g. gain of chromosome 3 detected in case E11 but not in ICH-ERMS-1, in cell lines (Fig. 1). Notably, SCMC-RM2 harbored unbalanced translocation of *PAX3/FOXO1*, which could not be detected in the primary tumor of ERMS (Fig. S3). However, unfortunately, since the RNA of the primary tumor was not available in this case, we could not examine the fusion gene status in the primary tumor.

ALK, GPC5 and IRS2 as candidate genes in amplified regions. Because gene amplification is an important mechanism for oncogene activation, we performed expression and mutation

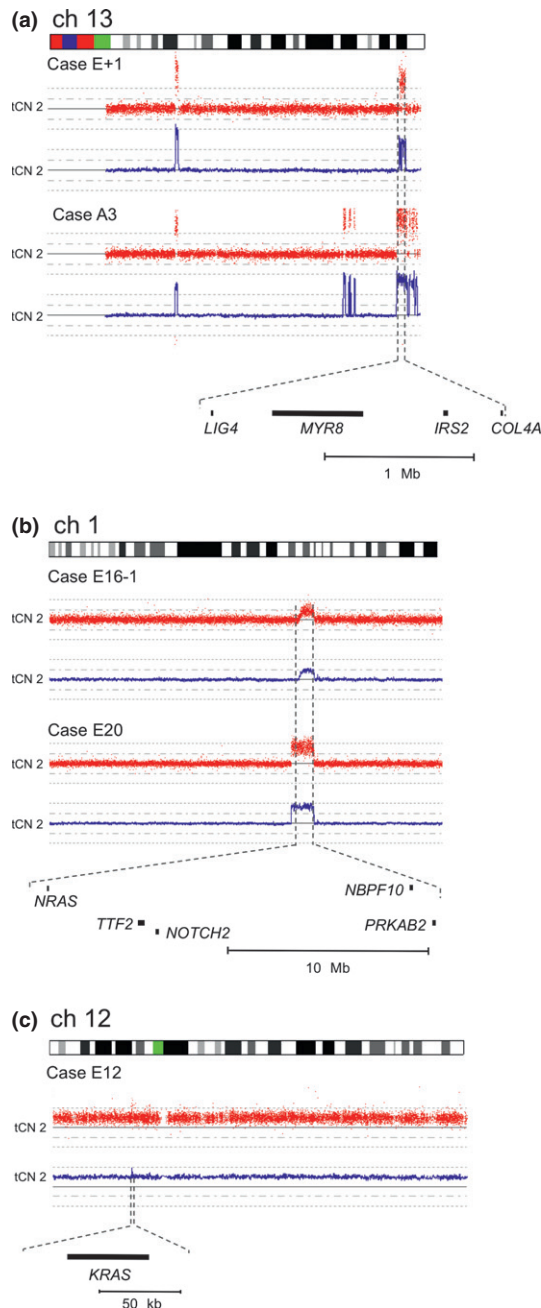


Fig. 4. Novel amplified regions detected in rhabdomyosarcoma (RMS). (a) Amplifications at genomic locus 13q33–q34 were detected in two patients. The minimal overlapping region of the two cases is indicated between the dotted lines, including the *IRS2* gene. Another common amplified region on the centromere side is the *FOXO1* locus, the fusion partner of *PAX3*. (b) The region containing the *NRAS* locus is amplified/gained in two ERMS cases. Representative genes are shown at the bottom of the figure. (c) *KRAS* is amplified in one ERMS case. ARMS, rhabdomyosarcoma with alveolar subtype; ERMS, rhabdomyosarcoma with embryonal subtype.

analyses of candidate genes: *ALK*, *GPC5* and *IRS2* located in amplified regions. Using RT-PCR, *ALK* expression was detected in 7/7 (100%) cell lines, 5/7 (71.4%) ARMS cases and 5/12 (41.7%) ERMS cases; *GPC5* was in 7/7 (100%) cell lines, 3/6 (50%) ARMS cases, 5/9 (55.6%) ERMS cases; and *IRS2* expression was in 7/7 (100%) cell lines, 4/5 (80%) ARMS cases, and 5/10 (50%) ERMS cases. In normal skeletal

muscle, only *IRS2* expression was detected among these genes. Because the RNA was not available from the cases with *ALK*, *GPC5* and/or *IRS2* amplifications, we could not evaluate the expression status in the cases concerned. Although no mutation was found in *ALK* and *GPC5*, a novel mutation (G54V) of *IRS2* was detected in SJRH18 (Fig. S4), which was not found in 60 healthy volunteers, not registered in dbSNP 137 (<http://www.ncbi.nlm.nih.gov/projects/SNP/>) and was not in 1000 genomes (<http://www.1000genomes.org/>). This single nucleotide change was scored as ‘probably damaging’ or ‘damaging’ by two computational prediction software, i.e. SIFT (<http://sift.jvci.org/>) and PolyPhen-2 (<http://genetics.bwh.harvard.edu/pph2/>).^(18,19)

Sensitivity of RMS-derived cell lines to ALK inhibition. To further evaluate the role of frequent ALK expression in RMS, we examined the effect of ALK inhibition on RMS cell proliferation using ALK inhibitors TAE684,⁽²⁰⁾ 2,4-PDD⁽²¹⁾ and crizotinib.⁽²¹⁾ Among the six ALK-expressing RMS cell lines examined, SJRH1 and SJRH30 were highly sensitive to these ALK inhibitors, showing IC₅₀ values comparable with those for LAN5, an ALK-mutated neuroblastoma cell line,⁽²²⁾ although the remaining four cell lines were relatively resistant (Fig. S5A). In neuroblastoma cells, correlation was observed between the levels of *ALK* expression and the response to ALK inhibitors.⁽²³⁾ Similarly, quantities of *ALK* mRNA seemed to correlate well with the IC₅₀ values for TAE684 and 2,4-PDD, but not for crizotinib in RMS (Fig. S5B,C).

Intratumor heterogeneity of RMS. In one ERMS case, we analyzed two separate blocks (E16-1, E16-2) of one biopsy specimen (3 × 2.3 × 1.6 cm) obtained from a bladder tumor. Although almost all chromosomal changes were shared in E16-1 and E16-2 (Fig. 5a), a number of regional specific changes were detected in each sample, for example, amplification at 1p13.2–q21.1, deletion at 1p31.3–p31.2 and 10q26.2–qter, biallelic gains at 15q13.3–qter and uniparental disomy at 20p13–p12.1 (Fig. 5b).

Discussion

With the use of the SNP array together with CNAG/AsCNAR, comprehensive allelic imbalances and subtle copy number changes could be accurately detected without paired normal samples, which allowed us to identify several genomic aberrations not previously known to be involved in RMS oncogenesis.

In accordance with previous studies, ERMS tumors were characterized by hyperploid copy number profiles with a combination of gains of chromosomes 2, 8 and 12. In contrast, ARMS shows near diploid profiles with more emphasized chromosomal losses, especially of 15q with a frequency of 45.5%. 15q LOH has been commonly found in other tumors, such as breast cancer, malignant mesothelioma and colorectal cancer,^(24–26) but not recognized in RMS (Fig S2).

Furthermore, 11p LOH has been observed characteristically in ERMS with a frequency of 80–100% in previous reports,^(4,27) but in addition to ERMS, high frequency of 11p LOH in ARMS was also observed in this present study. In the present cohort, four of five ARMS having 11p LOH represented genetic abnormalities of *PAX3/7* and *FOXO1*. This inconsistent result with previous publications^(4,27) might be due to the small number of patients in the present study or ethnic differences. Genetic alterations such as gain/amplification of *PAX3/FOXO1* loci was detected in 33.3% (2/6) of *PAX3-FOXO1*-positive tumors in the present cohort compared with 3% (1/31) using the 50K array, and 9% (7/79) using FISH in a previous report with a larger sample size.⁽²⁸⁾ There was no sampling bias for collecting tumor specimens, therefore these results might be attributed to not only sensitive detection of

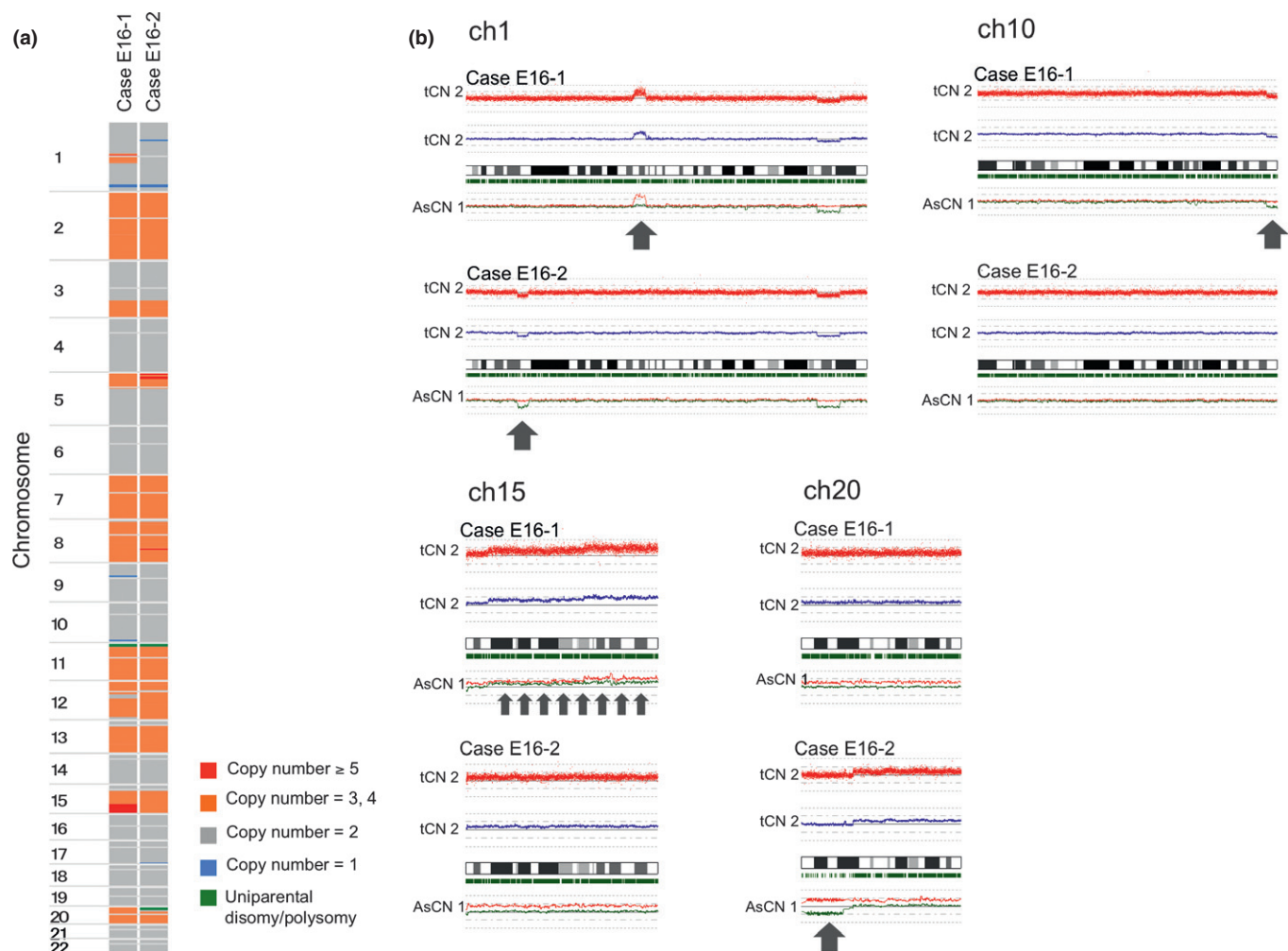


Fig. 5. Separated tumor specimens from the same tumor representing specific genomic aberrations. (a) Copy number profiles of the two samples are laid side by side for comparison. Each row indicates chromosome 1 to 22 and each column shows the affected region in each sample with the color legend. (b) Distinct regions between the two samples are indicated by the gray arrows. Green bars below each chromosome ideogram represent heterozygous single nucleotide polymorphism (SNP) calls. AsCN, allele specific copy number; tCN, total copy number.

LOH/amplification using high-density SNP array with CNAG/AsCNAR but also to the limited number of samples in the present study.

Several genetic prognostic factors in ARMS have been reported,^(29,30) but have been poorly defined in ERMS. In the present study we found that gain of 13q is significantly correlated with good patient outcome in ERMS. Although multivariate analyses in a larger cohort of patients are needed, gain of 13q is a possible candidate for being a novel prognostic factor for ERMS.

Amplifications/deletions were more informative for identifying gene targets. Among these, we found a novel recurrent amplified region at the *IRS2* locus on 13q. Amplification of the *IRS2* locus has been described in a subset of brain tumors,^(31,32) but not in RMS to date. Recent research has shown that overexpression of *IRS2* is associated with a poor outcome in RMS;⁽³³⁾ consistent with this, frequent expression of *IRS2* was predominantly observed in the present ARMS cohort. *IRS2*, a member of the insulin-like growth factor (IGF) pathway, is involved in resistance to apoptosis and increased metastatic potential in breast cancer,⁽³⁴⁾ and when overexpressed it enhances IGF-I-mediated AKT activation, prevents glucose-mediated apoptosis in human neuroblastoma cell lines⁽³⁵⁾

and leads to BAD phosphorylation preventing CASPASE3 cleavage.⁽³⁶⁾ Taken together, *IRS2* might contribute to tumorigenesis in a subset of RMS.

RAS mutations have been found in approximately 30% of ERMS,^(9,37) but amplifications of *KRAS* and *NRAS* have not been described previously in RMS. *RAS* amplifications are relatively common genetic alterations in various cancers, which often seem to indicate clinicopathological significance^(38,39) and contribute to secondary resistance to antitumor therapies.^(40,41) All three tumors with *RAS* amplifications were primary tumors of ERMS and therefore further studies including sequencing analyses are necessary to determine the clinicopathological impacts of *RAS* alterations on RMS.

Previously, *GPC5* in the 13q31 amplicon has been reported as a critical target for RMS,^(42,43) but another study has demonstrated that *miR-17-92* located in this region actually contributes to RMS development.⁽⁴⁴⁾ Although *GPC5* expression was absent in normal skeletal muscle, more than half of the RMS samples represented expressions of *GPC5* in this study, suggesting that aberrant *GPC5* activity might play a role in RMS oncogenesis.

Our high-resolution analysis also disclosed that seven ERMS samples probably had *PAX3/7-FOXO1* rearrangement. Among

the seven samples, one case could be re-evaluated using the histological findings and it was subsequently concluded that the patient had the alveolar subtype, suggesting the possible presence of alveolar cells in other fusion-positive ERMS. Likewise, *PAX3/FOXO1* unbalanced translocation was detected only in a cell line established from a relapsed tumor but not in the primary ERMS tumor, suggesting the presence of an ARMS component or balanced translocation of *PAX3/FOXO1*, which cannot be detected using a SNP array in the primary tumor.

ALK amplification found in case A1 was also intriguing from a therapeutic perspective. It has been reported that *ALK* is amplified in 6–17% of ARMS^(45,46) or altered in 19% of RMS cases.⁽⁴⁶⁾ In agreement with previous reports,^(45–47) we also demonstrated frequent *ALK* expression in RMS, predominantly in the ARMS subtype. Furthermore, despite no *ALK* expression in normal skeletal muscle, RMS tumors frequently represented expression of *ALK*, suggesting a role for aberrant *ALK* activity in the pathogenesis of RMS. In fact, we found that *ALK* inhibitors were effective in a portion of RMS cell lines with high *ALK* expression, suggesting a possible therapeutic application of *ALK* inhibitors for RMS. Compared with TAE684 and 2,4-PDD, the different pharmacological behavior of crizotinib might be related to MET inhibition, the specific activity of crizotinib, because the RMS cell lines examined also expressed MET to varying degrees.⁽⁴⁸⁾

Even in a single case, two separated specimens from the same tumor showed some distinct genomic changes. These events could not be explained by a different rate of nonaberrant cell admixture and therefore it suggests the presence of intratumor heterogeneity. This intratumor heterogeneity could present a considerable therapeutic challenge for RMS because treatment choices based on a biomarker present in a single

biopsy specimen might not be relevant. However, to provide an adequate assessment of intratumor heterogeneity, a larger number of tumor samples should be evaluated.

In summary, the present SNP array analysis revealed genome-wide genetic lesions including allelic imbalances in RMS, identified several candidate gene targets including *IRS2* and *ALK* and also suggested a therapeutic application of *ALK* inhibition to RMS. The results of the present study provide useful information for further analysis of RMS pathogenesis and in combination with data derived from other platforms, such as the next-generation sequencer, might lead to the discovery of promising candidate genes of RMS.

Acknowledgments

We are grateful to Ms Matsumura, Ms Hoshino, Ms Yin, Ms Saito, Ms Mori and Ms Ogino for their excellent technical assistance. We also express our appreciation to Dr A.T. Look (Harvard Medical University), Dr K. Yokomori (Graduate School of Medicine, University of Tokyo) and Dr A. Inoue (St Jude Children's Research Hospital) for their generous gifts of rhabdomyosarcoma cell lines, and to Astellas Pharma Inc. for the *ALK* inhibitors. This work was supported by: Research on Measures for Intractable Diseases, Health, and Labor Sciences Research Grants, Ministry of Health, Labour and Welfare; Research on Health Sciences focusing on Drug Innovation; the Japan Health Sciences Foundation; Core Research for Evolutional Science and Technology, Japan Science and Technology Agency; and Project for Development of Innovative Research on Cancer Therapeutics.

Disclosure Statement

The authors have no conflict of interest.

References

- Qualman SJ, Coffin CM, Newton WA *et al*. Intergroup Rhabdomyosarcoma Study: update for pathologists. *Pediatr Dev Pathol* 1998; **1**: 550–61.
- Barr FG. Gene fusions involving PAX and FOX family members in alveolar rhabdomyosarcoma. *Oncogene* 2001; **20**: 5736–46.
- Barr FG. Molecular genetics and pathogenesis of rhabdomyosarcoma. *J Pediatr Hematol Oncol* 1997; **19**: 483–91.
- Visser M, Sijmons C, Bras J *et al*. Allelotype of pediatric rhabdomyosarcoma. *Oncogene* 1997; **15**: 1309–14.
- Pandita A, Zielenska M, Thomer P *et al*. Application of comparative genomic hybridization, spectral karyotyping, and microarray analysis in the identification of subtype-specific patterns of genomic changes in rhabdomyosarcoma. *Neoplasia* 1999; **1**: 262–75.
- Gordon AT, Brinkschmidt C, Anderson J *et al*. A novel and consistent amplicon at 13q31 associated with alveolar rhabdomyosarcoma. *Genes Chromosom Cancer* 2000; **28**: 220–6.
- Bridge JA, Liu J, Weibolt V *et al*. Novel genomic imbalances in embryonal rhabdomyosarcoma revealed by comparative genomic hybridization and fluorescence *in situ* hybridization: an intergroup rhabdomyosarcoma study. *Genes Chromosom Cancer* 2000; **27**: 337–44.
- Bridge JA, Liu J, Qualman SJ *et al*. Genomic gains and losses are similar in genetic and histologic subsets of rhabdomyosarcoma, whereas amplification predominates in embryonal with anaplasia and alveolar subtypes. *Genes Chromosom Cancer* 2002; **33**: 310–21.
- Paulson V, Chandler G, Rakheja D *et al*. High-resolution array CGH identifies common mechanisms that drive embryonal rhabdomyosarcoma pathogenesis. *Genes Chromosom Cancer* 2011; **50**: 397–408.
- Nannya Y, Sanada M, Nakazaki K *et al*. A robust algorithm for copy number detection using high-density oligonucleotide single nucleotide polymorphism genotyping arrays. *Cancer Res* 2005; **65**: 6071–9.
- Yamamoto G, Nannya Y, Kato M *et al*. Highly sensitive method for genomewide detection of allelic composition in nonpaired, primary tumor specimens by use of affymetrix single-nucleotide-polymorphism genotyping microarrays. *Am J Hum Genet* 2007; **81**: 114–26.
- Chen Y, Takita J, Choi YL *et al*. Oncogenic mutations of *ALK* kinase in neuroblastoma. *Nature* 2008; **455**: 971–4.
- Okubo J, Takita J, Chen Y *et al*. Aberrant activation of *ALK* kinase by a novel truncated form *ALK* protein in neuroblastoma. *Oncogene* 2012; **31**: 4667–76.
- Mei R, Galipeau PC, Prass C *et al*. Genome-wide detection of allelic imbalance using human SNPs and high-density DNA arrays. *Genome Res* 2000; **10**: 1126–37.
- Iolascon A, Faienza MF, Coppola B *et al*. Analysis of cyclin-dependent kinase inhibitor genes (*CDKN2A*, *CDKN2B*, and *CDKN2C*) in childhood rhabdomyosarcoma. *Genes Chromosom Cancer* 1996; **15**: 217–22.
- Wachtel M, Dettling M, Koscielniak E *et al*. Gene expression signatures identify rhabdomyosarcoma subtypes and detect a novel t(2;2)(q35;p23) translocation fusing *PAX3* to *NCOA1*. *Cancer Res* 2004; **64**: 5539–45.
- Sumegi J, Streblov R, Frayer RW *et al*. Recurrent t(2;2) and t(2;8) translocations in rhabdomyosarcoma without the canonical *PAX-FOXO1* fuse *PAX3* to members of the nuclear receptor transcriptional coactivator family. *Genes Chromosom Cancer* 2010; **49**: 224–36.
- Kumar P, Henikoff S, Ng PC. Predicting the effects of coding non-synonymous variants on protein function using the SIFT algorithm. *Nat Protoc* 2009; **4**: 1073–81.
- Adzhubei IA, Schmidt S, Peshkin L *et al*. A method and server for predicting damaging missense mutations. *Nat Methods* 2010; **7**: 248–9.
- Galkin AV, Melnick JS, Kim S *et al*. Identification of NVP-TAE684, a potent, selective, and efficacious inhibitor of NPM-*ALK*. *Proc Natl Acad Sci U S A* 2007; **104**: 270–5.
- Choi YL, Soda M, Yamashita Y *et al*. *EML4-ALK* mutations in lung cancer that confer resistance to *ALK* inhibitors. *N Engl J Med* 2010; **363**: 1734–9.
- Bresler SC, Wood AC, Haglund EA *et al*. Differential inhibitor sensitivity of anaplastic lymphoma kinase variants found in neuroblastoma. *Sci Transl Med*. 2011; **3**: 108ra14.
- Duijkers FA, Gaal J, Meijerink JP *et al*. Anaplastic lymphoma kinase (*ALK*) inhibitor response in neuroblastoma is highly correlated with *ALK* mutation status, *ALK* mRNA and protein levels. *Cell Oncol (Dordr)*. 2011; **34**: 409–17.
- Fang M, Toher J, Morgan M, Davison J, Tannenbaum S, Claffey K. Genomic differences between estrogen receptor (ER)-positive and ER-negative

- human breast carcinoma identified by single nucleotide polymorphism array comparative genome hybridization analysis. *Cancer* 2011; **117**: 2024–34.
- 25 De Rienzo A, Balsara BR, Apostolou S, Jhanwar SC, Testa JR. Loss of heterozygosity analysis defines a 3-cM region of 15q commonly deleted in human malignant mesothelioma. *Oncogene* 2001; **20**: 6245–9.
 - 26 Sheffer M, Bacolod MD, Zuk O *et al*. Association of survival and disease progression with chromosomal instability: a genomic exploration of colorectal cancer. *Proc Natl Acad Sci U S A* 2009; **106**: 7131–6.
 - 27 Besnard-Guérin C, Newsham I, Winqvist R, Cavenee WK. A common region of loss of heterozygosity in Wilms' tumor and embryonal rhabdomyosarcoma distal to the D11S988 locus on chromosome 11p15.5. *Hum Genet* 1996; **97**: 163–70.
 - 28 Duan F, Smith LM, Gustafson DM *et al*. Genomic and clinical analysis of fusion gene amplification in rhabdomyosarcoma: a report from the Children's Oncology Group. *Genes Chromosom Cancer* 2012; **51**: 662–74.
 - 29 Missiaglia E, Williamson D, Chisholm J *et al*. PAX3/FOXO1 fusion gene status is the key prognostic molecular marker in rhabdomyosarcoma and significantly improves current risk stratification. *J Clin Oncol* 2012; **30**: 1670–7.
 - 30 Barr FG, Duan F, Smith LM *et al*. Genomic and clinical analyses of 2p24 and 12q13-q14 amplification in alveolar rhabdomyosarcoma: a report from the Children's Oncology Group. *Genes Chromosom Cancer* 2009; **48**: 661–72.
 - 31 Ehrbrecht A, Müller U, Wolter M *et al*. Comprehensive genomic analysis of desmoplastic medulloblastomas: identification of novel amplified genes and separate evaluation of the different histological components. *J Pathol* 2006; **208**: 554–63.
 - 32 Knobbe CB, Reifenberger G. Genetic alterations and aberrant expression of genes related to the phosphatidylinositol-3'-kinase/protein kinase B (Akt) signal transduction pathway in glioblastomas. *Brain Pathol* 2003; **13**: 507–18.
 - 33 Davicioni E, Anderson JR, Buckley JD, Meyer WH, Triche TJ. Gene expression profiling for survival prediction in pediatric rhabdomyosarcomas: a report from the children's oncology group. *J Clin Oncol* 2010; **28**: 1240–6.
 - 34 Nagle JA, Ma Z, Byrne MA, White MF, Shaw LM. Involvement of insulin receptor substrate 2 in mammary tumor metastasis. *Mol Cell Biol* 2004; **24**: 9726–35.
 - 35 Kim B, Feldman EL. Insulin receptor substrate (IRS)-2, not IRS-1, protects human neuroblastoma cells against apoptosis. *Apoptosis* 2009; **14**: 665–73.
 - 36 Stöhr O, Hahn J, Moll L *et al*. Insulin receptor substrate-1 and -2 mediate resistance to glucose-induced caspase-3 activation in human neuroblastoma cells. *Biochim Biophys Acta* 2011; **1812**: 573–80.
 - 37 Shukla NN, Ameer N, Yilmaz I *et al*. Oncogene mutation profiling of pediatric solid tumors reveals significant subsets of embryonal rhabdomyosarcoma and neuroblastoma with mutated genes in growth signaling pathways. *Clin Cancer Res* 2012; **18**: 748–57.
 - 38 Wagner PL, Stiedl AC, Wilbertz T *et al*. Frequency and clinicopathologic correlates of KRAS amplification in non-small cell lung carcinoma. *Lung Cancer* 2011; **74**: 118–23.
 - 39 Deng N, Goh LK, Wang H *et al*. A comprehensive survey of genomic alterations in gastric cancer reveals systematic patterns of molecular exclusivity and co-occurrence among distinct therapeutic targets. *Gut* 2012; **61**: 673–84.
 - 40 Misale S, Yaeger R, Hobor S *et al*. Emergence of KRAS mutations and acquired resistance to anti-EGFR therapy in colorectal cancer. *Nature* 2012; **486**: 532–6.
 - 41 Edwards J, Krishna NS, Witton CJ, Bartlett JM. Gene amplifications associated with the development of hormone-resistant prostate cancer. *Clin Cancer Res* 2003; **9**: 5271–81.
 - 42 Li F, Shi W, Capurro M, Filmus J. Glypican-5 stimulates rhabdomyosarcoma cell proliferation by activating Hedgehog signaling. *J Cell Biol* 2011; **192**: 691–704.
 - 43 Williamson D, Selve J, Gordon T *et al*. Role for amplification and expression of glypican-5 in rhabdomyosarcoma. *Cancer Res* 2007; **67**: 57–65.
 - 44 Reichek JL, Duan F, Smith LM *et al*. Genomic and clinical analysis of amplification of the 13q31 chromosomal region in alveolar rhabdomyosarcoma: a report from the Children's Oncology Group. *Clin Cancer Res* 2011; **17**: 1463–73.
 - 45 Corao DA, Biegel JA, Coffin CM *et al*. ALK expression in rhabdomyosarcomas: correlation with histologic subtype and fusion status. *Pediatr Dev Pathol* 2009; **12**: 275–83.
 - 46 van Gaal JC, Flucke UE, Roeffen MH *et al*. Anaplastic lymphoma kinase aberrations in rhabdomyosarcoma: clinical and prognostic implications. *J Clin Oncol* 2012; **30**: 308–15.
 - 47 Pillay K, Govender D, Chetty R. ALK protein expression in rhabdomyosarcomas. *Histopathology* 2002; **41**: 461–7.
 - 48 Chen Y, Takita J, Mizuguchi M *et al*. Mutation and expression analyses of the MET and CDKN2A genes in rhabdomyosarcoma with emphasis on MET overexpression. *Genes Chromosom Cancer* 2007; **46**: 348–58.

Supporting Information

Additional Supporting Information may be found in the online version of this article:

Fig. S1. Copy number changes detected using a high-density single nucleotide polymorphism array.

Fig. S2. Re-clustering of Figure 1 is performed for identification of prognosis-specific copy number changes in each subgroup.

Fig. S3. Comparison of copy number profiles between cell line SCMC-RM2 and the corresponding original tumor (case E23).

Fig. S4. Sequence trace from SJRH18 with IRS2 mutation (G54V).

Fig. S5. Efficacy of ALK inhibitors on cell growth of RMS cell lines.

Table S1. Primer sets used for PCR and RT-PCR.

Table S2. Copy number status of fusion gene detected using a single nucleotide polymorphism array.

Table S3. Minimal recurrent regions of gains and losses detected in 46 rhabdomyosarcoma tumors.